# Crystal Structures and Extended X-Ray Absorption Fine Structure Spectra of $[Fe\{O(CH_2CO_2)_2\}(H_2O)_2X]$ (X = Cl or Br)†

**Anne K. Powell,[a] John M. Charnock,[a] Annette C. Flood,[a] C. David Garner,*[,a] Michael J. Ware[a] and William Clegg[b]**

[a] *Department of Chemistry, The University of Manchester, Manchester M13 9PL, UK*

[b] *Department of Chemistry, The University, Newcastle upon Tyne NE1 7RU, UK*

The crystal structures of the complexes $[Fe\{O(CH_2CO_2)_2\}(H_2O)_2X]$ (X = Cl or Br) have been determined by X-ray diffraction. They are isostructural six-co-ordinate monomers, the only significant structural difference being the iron–halogen bond lengths: Fe–Cl 2.231(1) Å and Fe–Br 2.370(1) Å. In both cases the oxydiacetate ligand has a virtually planar skeleton of C and O atoms, is terdentate (with the ether oxygen atom *trans* to the halide) and occupies *meridional* positions of a slightly distorted octahedron which is completed by the two mutually *trans* water molecules. Iron and bromine K-edge extended X-ray absorption fine structure spectral data are described and discussed. Infrared spectra show both iron–halogen bond stretching vibrations. A nitrato-complex (X = $NO_3$) has also been prepared and characterised.

As part of a study of the co-ordination chemistry of iron(III) in aqueous media with oxygen-donor ligands we have prepared and characterised a number of iron(III) complexes of the ligand oxydiacetic acid, $O(CH_2CO_2H)_2 = H_2oda$. Although oda complexes of lanthanide and actinide elements have previously been structurally characterised,[1–3] and cadmium[4] and calcium[5] complexes are known, copper is the only transition metal for which structures of oda complexes have been reported.[6–8] Studies of equilibria in aqueous solution[9] have found the formation constant for the 1:1 $Fe^{III}$–oda complex to be log $\beta_1 = 5.04$, with no evidence for the formation of complexes of higher stoichiometric ratio. Iron(III) has a strong affinity for oxygen-donor ligands and iron–carboxylate interactions are very important in Nature.[10] As a contribution to the characterisation of examples of these systems, we have determined the X-ray crystal structures of two of the monomeric complexes which form in aqueous solutions of iron(III) and $H_2oda$ under favourable conditions. These are of interest because they are the precursors of a series of oxo-bridged oligomers which we believe form in aqueous solutions and which should, in turn, provide insights into other systems consisting of oligomeric and polymeric arrays of iron and oxygen centres.

## Experimental

*Materials.*—All chemicals employed were reagent-grade and used without further purification.

$[Fe(oda)(H_2O)_2Cl]$ **1**. *Method* 1. An aqueous solution (25 $cm^3$) of $FeCl_3$ (0.81 g, 5 mmol) was mixed with an aqueous solution (25 $cm^3$) of the free acid, $H_2oda$ (0.67 g, 5 mmol). Microcrystalline complex **1** began to form immediately. The product was filtered off and recrystallised from hot water.

*Method* 2. Aqueous solutions of $Fe_2(SO_4)_3$ (2.0 g, 5 mmol), $H_2oda$ (1.34 g, 10 mmol), and NaCl (0.58 g, 10 mmol) were mixed to give a total volume of 100 $cm^3$. Green crystals of **1** were isolated by filtration after 1 week (Found: C, 18.4; H, 3.0; Cl, 13.5; Fe, 22.2. $C_4H_8ClFeO_7$ requires C, 18.5; H, 3.1; Cl, 13.7; Fe, 21.5%).

† *Supplementary data available:* see Instructions for Authors, *J. Chem. Soc., Dalton Trans.*, 1992, Issue 1, pp. xx–xxv.

*Non-SI unit employed:* eV ≈ $1.60 \times 10^{-19}$ J.

$[Fe(oda)(H_2O)_2Br]$ **2**. This complex was obtained as dark brown crystals using Method 2 but adding NaBr (1.03 g, 10 mmol) in place of NaCl (Found: C, 15.7; H, 2.7; Br, 25.9; Fe, 18.2. $C_4H_8BrFeO_7$ requires C, 15.8; H, 2.7; Br, 26.3; Fe, 18.4%).

$[Fe(oda)(H_2O)_2(NO_3)]$ **3**. This complex was obtained using Method 1, substituting $Fe(NO_3)_3 \cdot 9H_2O$ (2.02 g, 5 mmol) in place of $FeCl_3$. Salmon-pink crystals formed from the reaction solution over a few days. They could not be recrystallised due to the formation of hydrolysis products (Found: C, 16.9; H, 2.8; Fe, 19.8; N, 4.7. $C_4H_8FeNO_{10}$ requires C, 16.8; H, 2.8; Fe, 19.5; N, 4.9%).

*X-Ray Crystallography.—Crystal data.* **1**, $C_4H_8ClFeO_7$, $M = 259.4$, orthorhombic, space group *Aba*2, $a = 8.943(1)$, $b = 10.943(1)$, $c = 8.648(1)$ Å, $U = 846.3$ Å$^3$, $Z = 4$, $D_c = 2.036$ g cm$^{-3}$, $F(000) = 524$, $\mu = 2.10$ mm$^{-1}$ for Mo-K$\alpha$ radiation ($\lambda = 0.710\,73$ Å), crystal size 0.25 × 0.27 × 0.42 mm. **2**, $C_4H_8BrFeO_7$, $M = 303.9$, orthorhombic, space group *Aba*2, $a = 9.023(1)$, $b = 10.893(1)$, $c = 8.737(1)$ Å, $U = 858.7$ Å$^3$, $Z = 4$, $D_c = 2.350$ g cm$^{-3}$, $F(000) = 596$, $\mu$(Mo-K$\alpha$) = 6.37 mm$^{-1}$, crystal size 0.38 × 0.38 × 0.54 mm.

*Data collection and reduction.* For complex **1** [for **2** in square brackets where different]: Stoe-Siemens diffractometer, $T = 293$ K, cell parameters from 2θ values of 32 reflections with $20 < 2\theta < 25°$, ω–θ scan mode, ω scan range 1.19° [1.02°] + α-doublet separation, scan time 14–56 s including background, $2\theta_{max}$ 50°, index range $h$ 0–11, $k$ 0–13, $l$ −10 to 10. Semiempirical absorption corrections were applied, based on sets of equivalent reflections measured at different azimuthal angles: transmission 0.392–0.425 [0.032–0.055]. No significant intensity variation was observed for three standard reflections. 750 [755] Reflections were measured, of which 742 [718] had $F > 4\sigma(F)$.

*Structure solution and refinement.*[11] Patterson and difference syntheses, blocked-cascade refinement to minimise $\Sigma w\Delta^2$, anisotropic thermal parameters for non-H atoms; H of $CH_2$ constrained to give C–H 0.96 Å, H–C–H 109.5°, $U$(H) = $1.2U_{eq}$(C); H of $OH_2$ subject to soft restraint O–H 0.87(1) Å with freely refined isotropic $U$. Weighting $w^{-1} = \sigma^2(F) + gF^2$, $g = 0.000\,09$ [0.000 65]. Extinction $x = 2.8(3) \times 10^{-6}$ [$9.1(8) \times 10^{-6}$] such that $F'_c = F_c/(1 + xF_c^2/\sin 2\theta)^{\frac{1}{4}}$. Polar axis direction ($z$) determined by refinement of η to 0.98(6) [1.11(4)].[12] 71 Parameters, $R = 0.016$ [0.027], $R' = (\Sigma w\Delta^2/\Sigma wF_o^2)^{\frac{1}{2}} = 0.023$ [0.039], maximum shift/e.s.d. = 0.005 [0.006],

**Table 1** Atomic coordinates ( $\times 10^4$) for complex **1**

| Atom | *x* | *y* | *z* |
|---|---|---|---|
| Fe | 5000 | 5000 | 5000 |
| Cl | 5000 | 5000 | 2421(1) |
| O(1) | 3694(2) | 6403(1) | 5611(2) |
| C(1) | 3500(2) | 6716(2) | 7012(2) |
| O(2) | 2737(1) | 7602(1) | 7418(2) |
| C(2) | 4266(2) | 5956(2) | 8243(3) |
| O(3) | 5000 | 5000 | 7425(3) |
| O(4) | 3180(1) | 3887(1) | 4998(3) |
| H(4a) | 3061(27) | 3417(19) | 4221(19) |
| H(4b) | 2879(32) | 3509(23) | 5829(20) |

**Table 2** Atomic coordinates ( $\times 10^4$) for complex **2**

| Atom | *x* | *y* | *z* |
|---|---|---|---|
| Fe | 5000 | 5000 | 5000 |
| Br | 5000 | 5000 | 7713(1) |
| O(1) | 6322(3) | 3614(2) | 4384(5) |
| C(1) | 6522(4) | 3288(3) | 2998(5) |
| O(2) | 7292(3) | 2415(2) | 2608(5) |
| C(2) | 5742(4) | 4052(3) | 1784(5) |
| O(3) | 5000 | 5000 | 2601(7) |
| O(4) | 6780(3) | 6140(3) | 5010(4) |
| H(4a) | 7095(62) | 6491(40) | 4173(34) |
| H(4b) | 6927(53) | 6443(38) | 5914(24) |

**Table 3** Bond lengths (Å) and angles (°)

| | **1** (X = Cl) | **2** (X = Br) |
|---|---|---|
| Fe–X | 2.231(1) | 2.370(1) |
| Fe–O(1) | 2.001(1) | 1.998(3) |
| Fe–O(3) | 2.098(3) | 2.096(6) |
| Fe–O(4) | 2.033(1) | 2.030(3) |
| O(1)–C(1) | 1.270(3) | 1.275(6) |
| C(1)–O(2) | 1.237(2) | 1.226(4) |
| C(1)–C(2) | 1.514(3) | 1.521(6) |
| C(2)–O(3) | 1.423(2) | 1.423(5) |
| O(4)–H(4a) | 0.853(19) | 0.873(35) |
| O(4)–H(4b) | 0.871(21) | 0.866(25) |
| X–Fe–O(3) | 180.0 | 180.0 |
| X–Fe–O(1) | 105.3(1) | 105.6(1) |
| O(1)–Fe–O(3) | 74.7(1) | 74.4(1) |
| X–Fe–O(4) | 90.0(1) | 89.7(1) |
| O(1)–Fe–O(4) | 89.6(1) | 89.5(1) |
| O(3)–Fe–O(4) | 90.0(1) | 90.3(1) |
| O(1)–Fe–O(1′) | 149.4(1) | 148.8(2) |
| O(4)–Fe–O(1′) | 90.4(1) | 90.7(1) |
| O(4)–Fe–O(4′) | 180.0(2) | 179.5(2) |
| Fe–O(1)–C(1) | 122.5(1) | 123.4(3) |
| O(1)–C(1)–O(2) | 123.8(2) | 124.1(4) |
| O(1)–C(1)–C(2) | 117.5(2) | 116.4(3) |
| O(2)–C(1)–C(2) | 118.7(2) | 119.5(4) |
| C(1)–C(2)–O(3) | 105.2(2) | 105.3(4) |
| Fe–O(3)–C(2) | 119.8(1) | 120.1(3) |
| C(2)–O(3)–C(2′) | 120.4(3) | 119.7(6) |
| Fe–O(4)–H(4a) | 117.5(15) | 121.4(32) |
| Fe–O(4)–H(4b) | 122.0(16) | 111.0(29) |
| H(4a)–O(4)–H(4b) | 109.1(20) | 123.1(39) |

The prime denotes an atom generated by two-fold rotation about the Fe–X bond.

mean = 0.001 [0.001]; slope of normal probability plot = 1.33 [1.11]; no features in final difference map outside the range −0.42 to +0.62 e Å$^{-3}$ [−0.49 to +0.83 e Å$^{-3}$]. Atomic coordinates are given in Tables 1 and 2, bond lengths and angles in Table 3.

Additional material available from the Cambridge Crystallographic Data Centre comprises H-atom coordinates and thermal parameters.

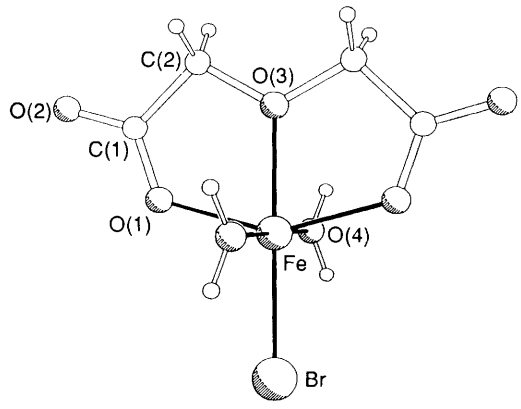


**Fig. 1** Molecular structure of complex **2** showing the atom numbering scheme, which is also used for **1**

*Physical Measurements.*—Infrared spectra of complexes **1**–**3** were recorded on a Perkin-Elmer PE 577 instrument from 4000 to 200 cm$^{-1}$ as Nujol and hexachlorobutadiene mulls sandwiched between CsI plates. Magnetic susceptibilities were measured using the Gouy method. Tubes were calibrated with $HgCo(NCS)_4$ and Pascal's constants were used in correcting the determined susceptibilities.

The extended X-ray absorption fine structure (EXAFS) spectra of complexes **1** and **2** were recorded in the transmission mode at the Synchrotron Radiation Source (SRS) at the Daresbury Laboratory. Iron K-edge spectra were measured on station 7.1 of the SRS using a Si(III) channel-cut monochromator. Data were collected from *ca.* 100 eV before to *ca.* 750 eV after the iron K-edge for both **1** and **2**; three scans were recorded and the data averaged. The bromine K-edge spectrum of **2** was recorded on station 9.2 of the SRS using a Si(220) double-crystal monochromator. Data were collected from *ca.* 100 eV before to *ca.* 1200 eV after the bromine K-edge; three scans were recorded and the data averaged. Each sample was mixed with boron nitride and the mixture finely ground to give an even dispersion of the compound in a powder of suitable X-ray absorbance. In each case the sample was at room temperature (*ca.* 293 K) during the measurements and the SRS was operating at 2 GeV with a current of *ca.* 150 mA. Background subtraction, normalisation and interpretation of the EXAFS was accomplished using single scattering in EXCURV 90,[13,14] with phase shifts calculated in the program using the default values of the parameters for calculation.

## Results and Discussion

*Crystal Structures.*—The two compounds are isostructural (Fig. 1), the only significant difference between the molecules being the Fe–Cl and Fe–Br bond lengths (Table 3). The oda dianion acts as a terdentate ligand, occupying three of the six co-ordination sites of the iron atom, the central ether oxygen atom lying *trans* to the halogen atom. The iron co-ordination geometry is distorted from ideal octahedral angles of 90° only by the restricted bite angle of the ligand. The O(3)–Fe–X line is a crystallographic two-fold rotation axis, imposing coplanarity on the bonds to O(3). All C and O atoms of the oda ligand lie close to a single plane [root mean square (r.m.s.) deviation = 0.045 Å for **1**, 0.046 Å for **2**].

The co-ordination of an almost planar oda ligand is also observed in the copper(II) complex $[Cu(oda)(terpy)]\cdot 2H_2O$[8] (terpy = 2,2′:6′,2″-terpyridyl) and in the calcium and cadmium complexes $[Ca(oda)(H_2O)_5]$[5] and $[Cd(oda)(H_2O)_3]$.[4] The ligand adopts a facial co-ordination in the other two copper(II) complexes which have been reported, $[Cu(oda)(bipy)(H_2O)]\cdot 4H_2O$[7] (bipy = 2,2′-bipyridyl) and $[Cu(oda)]\cdot 0.5H_2O$,[6] which results in a lengthening of the Cu–O (ether) bond and rather

**Table 4** Infrared bands ($cm^{-1}$) of $[Fe\{O(CH_2CO_2)_2\}(H_2O)_2X]$

| X | | | Tentative assignment |
|---|---|---|---|
| Cl | Br | $NO_3$ | |
| 3200– | 3200– | 3200– | ν(OH) and ν(CH) |
| 2800s(vbr) | 2800s(vbr) | 2800s(vbr) | |
| 1590s(br) | 1590s(br) | 1600s(br) | $\nu_{asym}(CO_2)$ |
| | | 1560m | $\nu_{asym}(NO_2)$ |
| 1458m | 1460m | 1465m | |
| 1435m | 1435m | 1425m | $\nu_{sym}(CO_2)$ |
| 1410m | 1410m | | and $\delta(CH_2)$ |
| 1345s | 1348s(sp) | 1350w | |
| 1302ms | 1305m | 1310s | |
| | | 1275s | $\nu_{sym}(NO_2)$ |
| 1225w | 1230w | 1235m | |
| 1120s(sp) | 1122s(sp) | 1110, 1105s | ν(C–O–C) |
| 1025s(sp) | 1028s(sp) | 1025s | $\nu_{sym}(NO)$ |
| 1000w(sp) | 1005w(sp) | 1005w(sh) | |
| 935s | 938s | 945s | |
| 860w | 860w | 850w(br) | |
| 810m | 792w | 802m(sp), | |
| | | 770m(sp) | $\delta_{sym}(NO_2)$ |
| 730mw | 730w | 740w(br) | |
| 595m | 595m | 593m | |
| 580m | 588m | 585m(sh) | ν(Fe–O) |
| 500m | 500m | 500m | |
| 465m | 465m | 450m | |
| | 392m | 380, 370m | |
| 385vs | | | ν(Fe–Cl) |
| 330m | 365m | 330m | |
| | 305vs(sp) | | ν(Fe–Br) |
| 305s | 290m | 315, 310, 305s | |
| | | 295, 285s | δ(O–Fe–O) |
| 230w | 230w | 230w | |

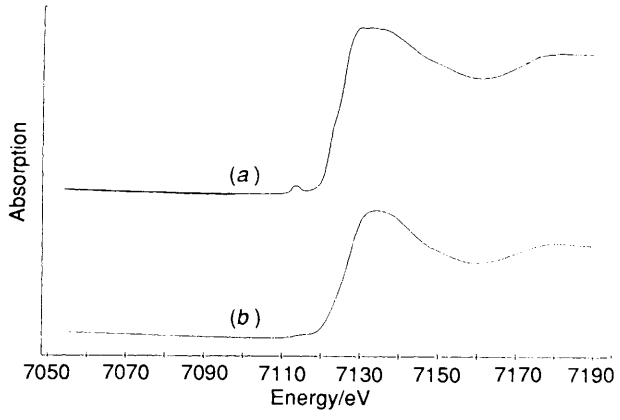


**Fig. 2** Comparison of the iron K-absorption edge and near-edge structure for complexes **1** (*a*) and **2** (*b*)

distorted structures. All these complexes have 1:1 metal to ligand ratios with the oda acting as a terdentate ligand. The bonding situation in the lanthanide and actinide complexes is naturally more complicated in view of the higher co-ordination numbers of the metal ions.[1–3]

*Infrared Spectra.*—The IR spectra of complexes **1** and **2** are remarkably similar, as indicated in Table 4, which also proposes approximate assignments. The major difference is in the 400–300 $cm^{-1}$ region. In the spectrum of **1** there is a very strong band at 385 $cm^{-1}$, which is assigned to an Fe–Cl stretching mode since this feature appears to be replaced by one at 305 $cm^{-1}$ in the spectrum of **2** where it is assigned to an Fe–Br stretching mode. The comparable frequencies of $[FeCl_4]^-$ and $[FeBr_4]^-$ are[15] 378 and 290 $cm^{-1}$, respectively. Although this region is

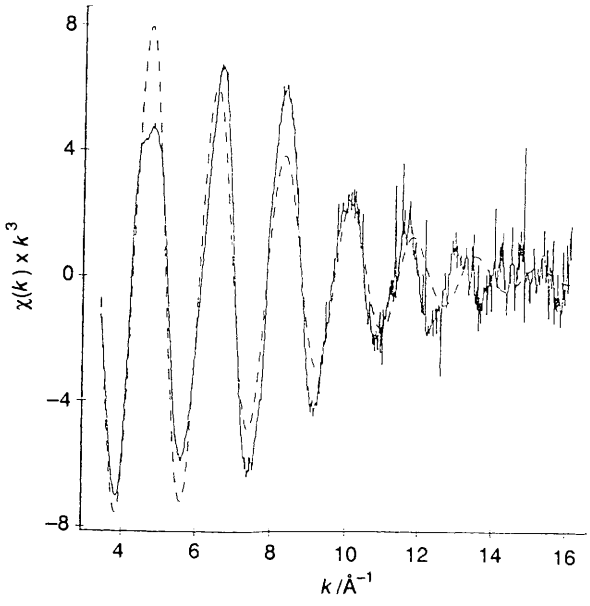


**Fig. 3** Iron K-edge EXAFS of complex **1** (——) compared to a simulation (– – –) involving back scattering from a shell of six oxygen atoms at 2.04 Å

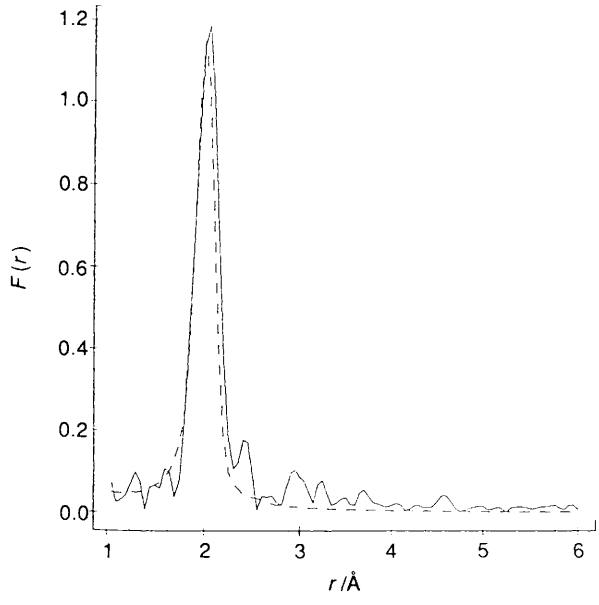


**Fig. 4** Fourier transforms of the EXAFS presented in Fig. 3

complicated by the presence of several ligands modes, a careful comparison of the spectra suggests that the assignments are correct. The spectrum of **3** (see Table 4) has the same ligand modes as those of **1** and **2** with the addition of absorptions characteristic of co-ordinated nitrate[15] at 1560, 1275 and 770 $cm^{-1}$. It seems probable that **3** possesses a structure analogous to that of **1** and **2**, but with a monodentate nitrate ligand in place of the halide.

*Magnetic Moments.*—The magnetic moments of complexes **1**, **2** and **3** at 298 K are 6.09, 6.12 and 5.55 $\mu_B$, respectively, typical of monomeric, high-spin octahedral iron(III) compounds.

*EXAFS Measurements.*—The low-energy regions (pre-edge, edge and near-edge) of the iron K-edge spectra of complexes **1** and **2** exhibit similar profiles (see Fig. 2). This is expected in view of the similar co-ordination geometry about the iron in both compounds. Each spectrum shows a weak pre-edge feature which is assigned to the 1s to 3d promotion of the

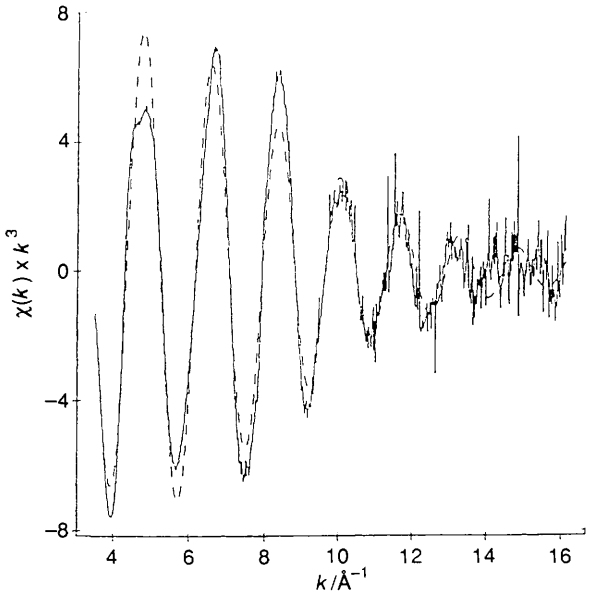


**Fig. 5** Iron K-edge EXAFS for complex **1** (——) compared to a simulation (– – –) involving back scattering from a shell of five oxygens at 2.03 Å and one chlorine at 2.19 Å

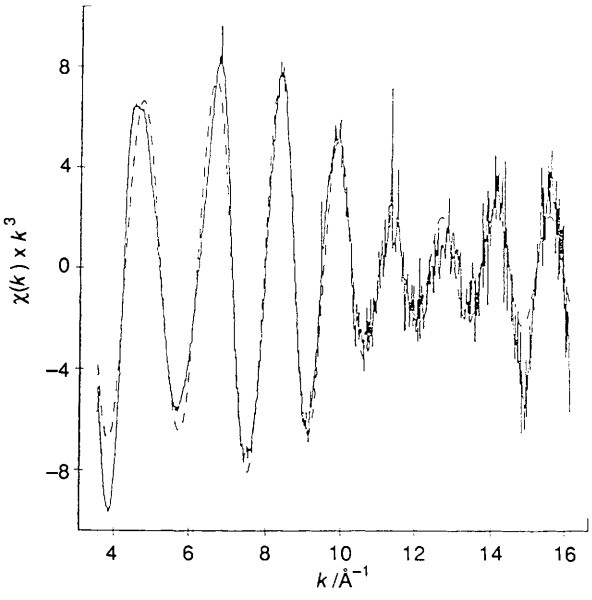


**Fig. 7** Iron K-edge EXAFS of complex **2** (——) compared to a simulation (– – –) involving back scattering from a shell of five oxygens at 2.02 Å and one bromine at 2.36 Å

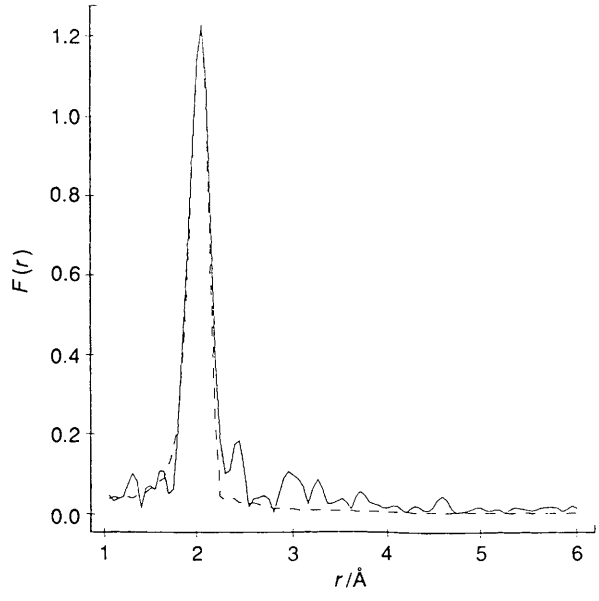


**Fig. 6** Fourier transforms of the EXAFS presented in Fig. 5

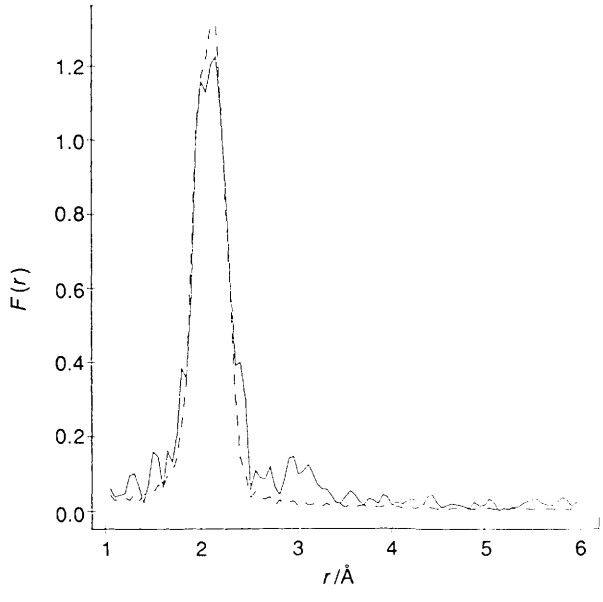


**Fig. 8** Fourier transforms of EXAFS presented in Fig. 7

**Table 5** Interpretations of EXAFS data recorded for **1** and **2**

| | | Interpretation | | | | |
|---|---|---|---|---|---|---|
| Compound | EXAFS | Atom | No. | Distance/Å | $\alpha^*$/Å$^2$ | Fit index |
| **1** | Fe-K-edge | O | 6 | 2.04 | 0.014 | 3.1 |
| | Fe-K-edge | O | 5 | 2.03 | 0.020 | 1.8 |
| | | Cl | 1 | 2.19 | 0.007 | |
| **2** | Fe-K-edge | O | 6 | 2.03 | 0.014 | 12.9 |
| | Fe-K-edge | O | 5 | 2.02 | 0.012 | 3.4 |
| | | Br | 1 | 2.36 | 0.006 | |
| | Br-K-edge | Fe | 1 | 2.35 | 0.006 | 2.2 |

* Debye–Waller parameter.

iron(III) centre. The intensity of this feature undoubtedly should relate to the symmetry of the iron atom and, therefore, may be able to provide a measure of the co-ordination number of an iron(III) complex. However, the different profiles and apparent intensities of the pre-edge feature seen for **1** and **2** indicate that such interpretations should be applied with caution.

The iron K-edge EXAFS of complex **1** (Fig. 3) approximates to that expected from the back scattering of a single shell of oxygen atoms at 2.04 Å. Thus, data of poor signal-to-noise ratio and a truncated range (say to 11 Å$^{-1}$), could fail to detect the presence of the chloride bound to the iron. We can trace the origin of this difficulty to the back-scattering contributions from the oxygen atoms at 2.03 Å and the chlorine at 2.23 Å from the iron being essentially $\pi$ out-of-phase throughout the spectral region measured. Therefore, the chlorine back-scattering contribution is primarily manifest in the *amplitude* of the EXAFS and can be taken up by variation in the Debye–Waller parameter associated with the dominant oxygen contribution.

However, a closer inspection of the EXAFS profiles in Fig. 3

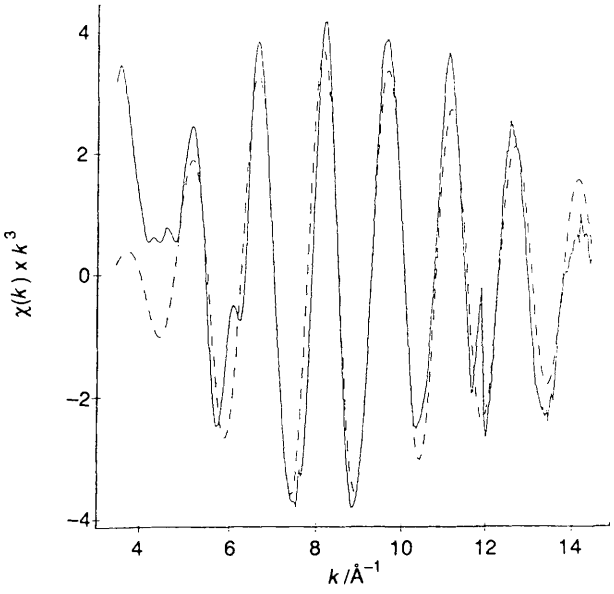


**Fig. 9** Bromine K-edge EXAFS of complex **2** (——) compared to a simulation (– – –) involving back scattering from an iron atom at 2.35 Å

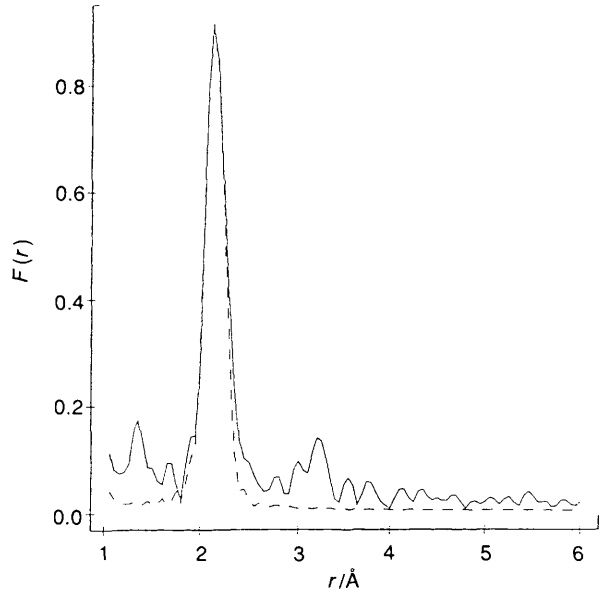


**Fig. 10** Fourier transforms of EXAFS presented in Fig. 9

reveals that, in addition to the amplitude discrepancies in the 3–11 $Å^{-1}$ region, phase discrepancies are manifest at higher $k$. The nature of the major deficiency in the treatment of the back scattering is apparent from the Fourier transform (Fig. 4) of the EXAFS of Fig. 3. Thus, an additional back-scattering contribution should be included at a distance that is slightly longer than that of the Fe–O shell. The inclusion of back scattering from a chlorine atom is statistically significant at the 1% level, using the criterion developed by Joyner *et al.*[16] and the fit index[13] (Table 5) is reduced from 3.1 to 1.8; the Fe–O and Fe–Cl distances of 2.03 and 2.19 Å are close to their respective crystallographic values of 2.03 and 2.23 Å. This interpretation of the EXAFS is shown in Fig. 5 and the Fourier transforms in Fig. 6. Further modest improvement in the agreement between the experimental and simulated EXAFS can be achieved by inclusion of a back-scattering contribution from the four carbon atoms [C(1), C(2), C(1′), C(2′)] centred at *ca.* 3 Å.

The iron K-edge EXAFS of complex **2** is well reproduced (Figs. 7 and 8) by simulations involving back-scattering contributions from one bromine and five oxygen atoms located from the iron at essentially the same distances as found by crystallography (Table 5). The bromine K-edge EXAFS of **2** is totally dominated by back scattering from the iron, as manifest in the Fourier transform by a peak at *ca.* 2.35 Å (Figs. 9 and 10).

A conclusion apparent from these EXAFS studies is that detection of the co-ordination of a ligand to a metal centre is greatly advantaged if it is possible to record the EXAFS associated with the absorption edge of that putative ligand atom.

## Acknowledgements

We thank the SERC for a research grant (to W. C.) towards crystallographic equipment, for the award of a Research Studentship (to A. C. F) and for the provision of facilities at the Daresbury Laboratory. A. K. P. thanks the Victoria University of Manchester for the award of a Rona Robinson Research Studentship.

## References

1 J. Albertsson, *Acta Chem. Scand.*, 1968, **22**, 1563; 1970, **24**, 3527; N. G. Vannerberg and J. Albertsson, *Acta Chem. Scand.*, 1965, **19**, 1760; J. Albertsson and I. Elding, *Acta Crystallogr., Sect. B*, 1976, **32**, 3066; *Acta Chem. Scand., Ser. A*, 1977, **31**, 21; I. Elding, *Acta Chem. Scand, Ser. A*, 1976, **30**, 649; 1977, **31**, 75.
2 F. R. Fronczek, A. K. Banerjee, S. F. Watkins and R. W. Schwartz, *Inorg. Chem.*, 1981, **20**, 2745.
3 G. Bombieri, R. Graziani and E. Forsellini, *Inorg. Nucl. Chem. Lett.*, 1973, **9**, 551; G. Bombieri, U. Croatto, R. Graziani, E. Forsellini and L. Magon, *Acta Crystallogr., Sect. B*, 1974, **30**, 407; R. Graziani, G. A. Battiston, U. Casellato and G. Sbrignadello, *J. Chem. Soc., Dalton Trans.*, 1983, 1; F. Benetollo, G. Bombieri, G. Tomat, C. B. Castellani, A. Cassol and P. di Bernardo, *Inorg. Chim. Acta*, 1984, **95**, 251.
4 C. E. Boman, *Acta Crystallogr., Sect. B*, 1977, **33**, 834, 838, 1529.
5 V. A. Uchtman and R. P. Oertel, *J. Am. Chem. Soc.*, 1973, **95**, 1082.
6 S. H. Whitlow and G. Davey, *J. Chem. Soc., Dalton Trans.*, 1975, 1228.
7 R. P. Bonomo, E. Rizzarelli, N. Bresciani-Pahor and G. Nardin, *Inorg. Chim. Acta*, 1981, **54**, 17.
8 N. Bresciani-Pahor, G. Nardin, R. P. Bonomo and E. Rizzarelli, *J. Chem. Soc., Dalton Trans.*, 1983, 1797.
9 A. Napoli, *J. Inorg. Nucl. Chem.*, 1972, **34**, 987.
10 Proceedings of the Fifth International Conference on Bioinorganic Chemistry, *J. Inorg. Biochem.*, 1991, **43**, 524–569.
11 G. M. Sheldrick, SHELXTL, an integrated system for solving, refining and displaying crystal structures from diffraction data, University of Göttingen, 1978.
12 D. Rogers, *Acta Crystallogr., Sect. A*, 1981, **37**, 734.
13 SERC Daresbury Laboratory EXCURV 90 Program, N. Binsted, J. W. Campbell, S. J. Gurman and P. C. Stephenson, 1990.
14 S. J. Gurman, N. Binsted and I. Ross, *J. Phys. C.*, 1984, **17**, 143.
15 K. Nakamoto, *Infrared and Raman Spectra of Inorganic and Coordination Compounds*, Wiley, New York, 1978.
16 R. W. Joyner, K. J. Martin and P. Meehan, *J. Phys. C.*, 1987, **20**, 4005.

*Received* 19*th August* 1991; *Paper* 1/04340D